Rate Maximization of UAV-Assisted Ambient Backscatter Communications

Xiaoyu Wu, Xu Jiang, *Member, IEEE,* Bo Li, *Member, IEEE,* Nan Zhao, *Senior Member, IEEE,* Peihua Li, *Member, IEEE,* Yonghui Li, *Fellow, IEEE,* and Arumugam Nallanathan, *Fellow, IEEE*

***Abstract*—Unmanned aerial vehicle (UAV) has been extensively deployed to improve wireless coverage due to its high mobility, while ambient backscatter communication has the advantage in improving the energy efficiency. Thus, UAV can be employed to assist ambient backscatter communications when the ground source is unavailable. In this correspondence, a UAV-assisted ambient backscatter communication scheme is investigated to maximize the average transmission rate of backscatter users by jointly optimizing the user scheduling, transmit power and UAV's trajectory. The formulated problem is non-convex with integer variables, which is solved by a three-stage iterative algorithm. The user scheduling is first approximately solved. To accelerate the convergence, a coarse optimization scheme is then proposed to obtain the preliminary transmit power and trajectory. Finally, a fine optimization scheme is adopted to improve the accuracy. Simulation results show that the backscatter rate can be effectively enhanced by the proposed scheme.**

***Index Terms*—Ambient backscatter communication, rate maximization, trajectory optimization, unmanned aerial vehicle.**

I. Introduction

Unmanned aerial vehicle (UAV) aided wireless communication has been widely investigated, which has the advantage of extending terrestrial wireless coverage and enhancing capacity [1], [2]. Benefiting from the swift deployment and high possibility of line-of-sight (LoS) air-ground links, UAV-assisted communications have been studied in various applications, including surveillance for public safety, data relaying between isolated areas, as well as data gathering and dissemination for remote Internet of Things (IoT) devices [3], [4].

Several techniques has been investigated to achieve energy sustainability, such as integrated data and energy transfer [5], [6] and ambient backscatter communication (AmBC) [7]. AmBC is able to provide wireless transmission by exploiting ambient radio frequency (RF) signals from existing infrastructures, such as TV towers and base stations [8]. Since the information is modulated by reflecting the incident signal, mobile devices can transmit data without power-hungry RF transmitters, which is energy-efficient and cost-saving. Thus, AmBC is deemed as a promising technology to support future low-power IoT applications. In UAV-assisted networks, the wireless signal emitted by the UAV can be regarded as an excellent RF resource for AmBC due to the LoS channels. Accordingly, UAV and AmBC can be combined for better performance.

Due to the above-mentioned advantages, UAV-assisted backscatter communications have been extensively investigated. In [9], UAV was employed by Yang *et al*. to gather data from multiple backscatter devices. A UAV-enabled backscatter system was proposed by Tran *et al*., where the UAV was utilized for active relaying and passive backscattering simultaneously [10]. By exploiting LoS air-ground channels, the RF signals transmitted by UAV can be leveraged for AmBC [11], [12]. For example, the UAV can work as both RF emitter and relay to assist the AmBC [11]. In [12], an energy-efficient scheme was proposed by Han *et al*. for UAVs to serve multiple backscatter devices. By employing the UAV as RF source, the passive intelligent reflecting surface can send its own message via AmBC [13]. In IoT networks, the UAV can be deployed for both RF emitting and data gathering. This scenario was investigated in [14], [15], where the UAV's mobility was exploited to improve the performance. Taking the channel fading into consideration, the outage performance of UAV-assisted AmBC was analyzed in [16]. In the above-mentioned literature, the main task of UAV is to support the AmBC. Nevertheless, the UAV can support the air-ground communication and AmBC simultaneously, which has not been fully investigated.

Motivated by the above discussions, a UAV-assisted AmBC system is investigated in this correspondence, where the UAV serves multiple ground users, and its transmitted signal is also leveraged for AmBC. Aiming at maximizing the average rate of backscatter pairs while satisfying rate constraints of ground users, we focus on the joint optimization of user scheduling, transmit power and UAV's trajectory. More importantly, we propose a coarse optimization and a fine optimization to accelerate the convergence and reduce the complexity. Overall, a three-stage iterative algorithm is proposed to acquire an approximate solution.

II. System Model and Problem Formulation

A. System Model

Consider the UAV-assisted AmBC system demonstrated in Fig. 1, where K ground users and M pairs of backscatter

X. Wu, N. Zhao and P. Li are with the School of Information and Communication Engineering, Dalian University of Technology, Dalian 116024, China (email: wuxiaoyu@mail.dlut.edu.cn; zhaonan@dlut.edu.cn, peihuali@dlut.edu.cn).

X. Jiang and B. Li are with the School of Information Science and Engineering, Harbin Institute of Technology (Weihai), Weihai, 264209, China. (e-mail: xjiang@hit.edu.cn; libo1983@hit.edu.cn)

Y. Li is with the School of Electrical and Information Engineering, University of Sydney, Sydney, NSW 2006, Australia (e-mail: yonghui.li@sydney.edu.au).

A. Nallanathan is with the School of Electronic Engineering and Computer Science, Queen Mary University of London, London E1 4NS, U.K. (e-mail: a.nallanathan@qmul.ac.uk).

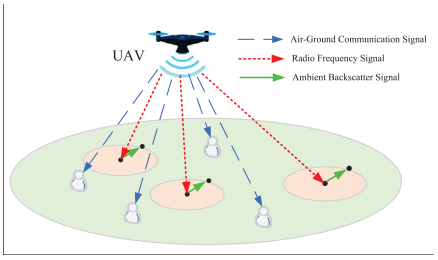

Fig. 1. UAV-assisted ambient backscatter communications.

users are served by the UAV simultaneously. Since the air-ground channel is LoS dominated, the single antenna scenario is considered. The horizontal coordinate of the kth ground user is represented as $\mathbf{w}_k = [x_{w,k}, y_{w,k}]^{\mathrm{T}} \in \mathbb{R}^{2\times 1}, k \in \mathcal{K} \triangleq \{1, 2, \ldots, K\}$. Similarly, the coordinates of the mth backscatter transmitter and the mth backscatter receiver are expressed as $\mathbf{a}_m = [x_{a,m}, y_{a,m}]^{\mathrm{T}} \in \mathbb{R}^{2\times 1}$ and $\mathbf{b}_m = [x_{b,m}, y_{b,m}]^{\mathrm{T}} \in \mathbb{R}^{2\times 1}$, $m \in \mathcal{M} \triangleq \{1, 2, \ldots, M\}$, respectively. Each backscatter transmitter and its corresponding receiver is assumed to have a fixed distance d_0. The UAV is assumed to fly at a fixed height of H and finally returns to its initial location within the duration of T, which can be divided into N time slots. The value of N is a tradeoff between the accuracy and complexity. The horizontal coordinate of UAV is $\mathbf{u}[n] = [x_u[n], y_u[n]]^T$, $n \in \mathcal{N} \triangleq \{1, 2, \ldots, N\}$, and the maximum flying distance of UAV in each slot is D. Thus, the UAV trajectory should satisfy

$$\|\mathbf{u}[n+1] - \mathbf{u}[n]\| \le D, \; n = 1, 2, \cdots, N-1, \tag{1}$$

$$\mathbf{u}[1] = \mathbf{u}[N]. \tag{2}$$

According to [17], if the UAV is deployed high enough, LoS air-ground link can be achieved. Thus, the Frris model is employed for the air-ground path loss. The channel gain between the UAV and the kth ground user can be written as

$$h_{uk}[n] = \frac{\beta_0}{\left(H^2 + \|\mathbf{u}[n] - \mathbf{w}_k\|^2\right)}, \; k \in \mathcal{K}, \; n \in \mathcal{N}, \tag{3}$$

where β_0 denotes the channel gain at 1 m.

Since the reflected power of AmBC is low, the interference from AmBC is ignored for ease of analysis. Thus, the signal-to-noise ratio (SNR) of the kth ground user is denoted as

$$\gamma_{w,k}[n] = \frac{p[n]\, h_{uk}[n]}{\sigma^2} = \frac{p[n]\, \beta_0}{(\|\mathbf{u}[n] - \mathbf{w}_k\|^2 + H^2)\sigma^2}, \tag{4}$$

where $p[n]$ is the UAV transmit power, σ^2 is the additive white Gaussian noise (AWGN) power.

The user scheduling is denoted by $\theta_k[n] \in \{0, 1\}$, $n \in \mathcal{N}$, $k \in \mathcal{K}$. $\theta_k[n] = 1$ indicates that the kth user is served by the UAV in time slot n, otherwise, $\theta_k[n] = 0$. To avoid interference, we assume that the UAV can communicate with no more than one ground user during one time slot, i.e.

$$\sum\nolimits_{k=1}^{K} \theta_k[n] \le 1, \; n \in \mathcal{N}. \tag{5}$$

Then, the average rate of the kth ground user is denoted as

$$\bar{R}_{w,k} = \frac{1}{N} \sum\nolimits_{n=1}^{N} \theta_k[n] \log_2(1 + \gamma_{w,k}[n]). \tag{6}$$

Assume that a minimum average rate R_0 is required for the kth ground user. Then, we have $\bar{R}_{w,k} \ge R_0, \; k \in \mathcal{K}$.

Each backscatter transmitter reflects the signal from UAV, through which it sends its own message to its corresponding receiver. The interference of other backscatter users can be ignored due to their long distance and low transmit power. Thus, only the interference from the UAV is considered. According to the analyses and experiments in [18], the interference from the RF source can be attenuated up to 50 dB by shifting the backscatter frequency away from the UAV's signal frequency. By this means, only a small part of interference power is left at each backscatter receiver, which is denoted by a coefficient μ [16]. Thus, the signal-to-interference-plus-noise ratio (SINR) at the mth backscatter receiver is expressed as

$$\gamma_{b,m}[n] = \frac{\frac{p[n]\beta_0^2 \varsigma}{(\|\mathbf{u}[n]-\mathbf{a}_m\|^2+H^2)d_0^\alpha}}{\frac{\mu p[n]\beta_0}{(\|\mathbf{u}[n]-\mathbf{b}_m\|^2+H^2)} + \sigma^2}, \tag{7}$$

where $\varsigma \sim \exp(1)$ denotes the Rayleigh fading. $\alpha > 2$ is the path-loss exponent. Thus, the ergodic rate of the mth backscatter user in time slot n is expressed as

$$\tilde{R}_{b,m}[n] = \mathbb{E}_\varsigma\left[\log_2\left(1 + \gamma_{b,m}[n]\right)\right] \tag{8a}$$

$$\le \log_2\left(1 + \frac{\frac{p[n]\beta_0^2 \mathbb{E}_\varsigma[\varsigma]}{(\|\mathbf{u}[n]-\mathbf{a}_m\|^2+H^2)d_0^\alpha}}{\frac{\mu p[n]\beta_0}{(\|\mathbf{u}[n]-\mathbf{b}_m\|^2+H^2)} + \sigma^2}\right) \tag{8b}$$

$$= \log_2\left(1 + \frac{\frac{p[n]\beta_0^2}{(\|\mathbf{u}[n]-\mathbf{a}_m\|^2+H^2)d_0^\alpha}}{\frac{\mu p[n]\beta_0}{(\|\mathbf{u}[n]-\mathbf{b}_m\|^2+H^2)} + \sigma^2}\right) = R_{b,m}[n], \tag{8c}$$

where $\mathbb{E}_\varsigma[\cdot]$ in (8a) is the mathematical expectation with respect to ς, and (8b) results from Jensen's inequality. To simplify the analysis in the following, the upper bound obtained in (8c) is adopted as the maximum achievable rate for AmBC.

B. Problem Formulation

To maximize the average backscatter transmission rate, the ground user scheduling $\mathbf{\Theta} = \{\theta_k[n], \; k \in \mathcal{K}, \; n \in \mathcal{N}\}$, transmit power $\mathbf{P} = \{p[n], \; n \in \mathcal{N}\}$ and UAV trajectory $\mathbf{U} = \{\mathbf{u}[n], \; n \in \mathcal{N}\}$ should be jointly optimized. The optimization problem can be expressed as

$$\max_{\mathbf{\Theta},\mathbf{P},\mathbf{U}} \min_{m} \frac{1}{N} \sum\nolimits_{n=1}^{N} R_{b,m}[n] \tag{9a}$$

$$s.t. \quad \bar{R}_{w,k} \ge R_0, \; k \in \mathcal{K}, \tag{9b}$$

$$\frac{1}{N} \sum\nolimits_{n=1}^{N} p[n] \le p_0, \tag{9c}$$

$$p[n] \ge 0, \; n \in \mathcal{N}, \tag{9d}$$

$$p[n] \le 5p_0, \; n \in \mathcal{N}, \tag{9e}$$

$$\|\mathbf{u}[n+1] - \mathbf{u}[n]\| \le D, n = 1, 2, \cdots, N-1, \tag{9f}$$

$$\mathbf{u}[1] = \mathbf{u}[N], \tag{9g}$$

$$\theta_k[n] \in \{0, 1\}, \; k \in \mathcal{K}, \; n \in \mathcal{N}, \tag{9h}$$

$$\sum\nolimits_{k=1}^{K} \theta_k[n] \le 1, \; n \in \mathcal{N}. \tag{9i}$$

where p_0 is the maximum average transmit power, and (9c) denotes the power constraint. (9) is a complicated non-convex problem, which is challenging to tackle.

III. Iterative Algorithm for the Optimization

To make the problem (9) tractable, it is divided into two sub-problems. For the first sub-problem, it is solved by relaxing the integer variable $\theta_k[n]$ into a continuous one. For the second one, a two-stage scheme including coarse optimization and fine optimization is proposed to accelerate the convergence. The three stages are performed alternately in an iterative manner to obtain an effective solution to the original problem.

A. User Scheduling Optimization

First, the binary variables in (9h) are approximated by the following continuous ones as

$$0 \le \hat{\theta}_k[n] \le 1,\ n \in \mathcal{N},\ k \in \mathcal{K}. \tag{10}$$

The user scheduling is targeted at satisfying the rate requirement of UAV-served ground users. Therefore, the objective function is maximizing their average rate. With continuous variables $\hat{\mathbf{\Theta}} = \{\hat{\theta}_k[n],\ k \in \mathcal{K},\ n \in \mathcal{N}\}$, the user scheduling optimization in (9) is rewritten as

$$\max_{\hat{\mathbf{\Theta}}}\ \min_{k}\ \frac{1}{N}\sum\nolimits_{n=1}^{N} \hat{\theta}_k[n]\log_2(1+\gamma_{w,k}[n]) \tag{11a}$$

$$s.t.\ \ \sum\nolimits_{k=1}^{K} \hat{\theta}_k[n] \le 1,\ n \in \mathcal{N}, \tag{11b}$$

$$0 \le \hat{\theta}_k[n] \le 1,\ n \in \mathcal{N},\ k \in \mathcal{K}. \tag{11c}$$

For this linear programming, we can solve it by CVX.

B. Coarse Optimization of Transmit Power and Trajectory

To accelerate the convergence, a coarse optimization is proposed to obtain the pre-optimized results. In (7), we ignore the interference from UAV, and the SNR of the mth backscatter receiver is expressed as

$$\hat{\gamma}_{b,m}[n] = \frac{\beta_0^2 \varsigma}{\left(\frac{\|\mathbf{u}[n]-\mathbf{a}_m\|^2+H^2}{p[n]}\right) d_0^{\alpha}\sigma^2}. \tag{12}$$

Similar to (8), the upper bound of the ergodic rate is adopted as

$$\begin{aligned}\hat{R}_{b,m}[n] &= \log_2\left(1+\frac{\beta_0^2}{\left(\frac{\|\mathbf{u}[n]-\mathbf{a}_m\|^2+H^2}{p[n]}\right) d_0^{\alpha}\sigma^2}\right) \\ &\ge \mathbb{E}_{\varsigma}\left[\log_2\left(1+\hat{\gamma}_{b,m}[n]\right)\right].\end{aligned} \tag{13}$$

With fixed $\hat{\mathbf{\Theta}}$, the joint optimization of $\mathbf{P}$ and $\mathbf{U}$ in (9) can be given as

$$\max_{\mathbf{P},\mathbf{U}}\ \min_{m}\ \frac{1}{N}\sum\nolimits_{n=1}^{N} \hat{R}_{b,m}[n] \tag{14a}$$

$$s.t.\ \ \bar{R}_{w,k} \ge R_0,\ k \in \mathcal{K}, \tag{14b}$$

$$(9c),\ (9d),\ (9e),\ (9f),\ (9g). \tag{14c}$$

For ease of expression, we define $\delta_m[n] = \frac{\|\mathbf{u}[n]-\mathbf{a}_m\|^2+H^2}{p[n]}$ and $\delta_m^r[n] = \frac{\|\mathbf{u}^r[n]-\mathbf{a}_m\|^2+H^2}{p^r[n]}$, where $p^r[n]$ and $\mathbf{u}^r[n]$ are the transmit power and trajectory in the rth iteration, respectively. Although $\hat{R}_{b,m}[n]$ is not convex with respect to $p[n]$ and $\mathbf{u}[n]$, it is convex with $\delta_m[n]$. Since the first-order Taylor expansion of a convex function is its global lower bound, we have

$$\hat{R}_{b,m}[n] \ge A_m^r[n] + B_m^r[n]\left(\delta_m[n]-\delta_m^r[n]\right) = \hat{R}_{b,m}^{lb}[n], \tag{15}$$

where

$$A_m^r[n] = \log_2\left(1+\frac{\beta_0^2}{\delta_m^r[n] d_0^{\alpha}\sigma^2}\right), \tag{16}$$

$$B_m^r[n] = -\frac{\frac{\beta_0^2}{(\delta_m^r[n])^2 d_0^{\alpha}\sigma^2}\log_2 e}{1+\frac{\beta_0^2}{\delta_m^r[n] d_0^{\alpha}\sigma^2}}. \tag{17}$$

For the non-convex constraint in (14b), we define the following convex expression $R_{w,k}[n] = \log_2\left(1+\frac{\beta_0}{\zeta_k[n]\sigma^2}\right)$, where $\zeta_k[n] = \frac{\|\mathbf{u}[n]-\mathbf{w}_k\|^2+H^2}{p[n]}$. Similarly, by defining $\zeta_k^r[n] = \frac{\|\mathbf{u}^r[n]-\mathbf{w}_k\|^2+H^2}{p^r[n]}$, the lower bound of $R_{w,k}[n]$ can be given by the following first-order inequality as

$$R_{w,k}[n] \ge C_k^r[n] + D_k^r[n]\left(\zeta_k[n]-\zeta_k^r[n]\right) = R_{w,k}^{lb}[n], \tag{18}$$

where

$$C_k^r[n] = \log_2\left(1+\frac{\beta_0}{\zeta_k^r[n]\sigma^2}\right), \tag{19}$$

$$D_k^r[n] = -\frac{\frac{\beta_0}{\left(\zeta_k^r[n]\right)^2\sigma^2}\log_2 e}{1+\frac{\beta_0}{\zeta_k^r[n]\sigma^2}}. \tag{20}$$

Thus, (14) can be approximately written as

$$\max_{\mathbf{P},\mathbf{U}}\ \min_{m}\ \frac{1}{N}\sum\nolimits_{n=1}^{N} \hat{R}_{b,m}^{lb}[n] \tag{21a}$$

$$s.t.\ \ \frac{1}{N}\sum\nolimits_{n=1}^{N} \hat{\theta}_k[n] R_{w,k}^{lb}[n] \ge R_0,\ k \in \mathcal{K}, \tag{21b}$$

$$(9c),\ (9d),\ (9e),\ (9f),\ (9g), \tag{21c}$$

which is convex and can be solved with polynomial complexity. After solving (21), the obtained coarse optimized transmit power and trajectory are denoted as $\bar{\mathbf{P}}$ and $\bar{\mathbf{U}}$, respectively.

C. Fine Optimization of Transmit Power and Trajectory

The interference from UAV is taken into consideration in the fine optimization. With fixed user scheduling $\hat{\mathbf{\Theta}}$, the problem (9) is written as

$$\max_{\mathbf{P},\mathbf{U}}\ \min_{m}\ \frac{1}{N}\sum\nolimits_{n=1}^{N} R_{b,m}[n] \tag{22a}$$

$$s.t.\ \ \bar{R}_{w,k} \ge R_0,\ k \in \mathcal{K}, \tag{22b}$$

$$(9c),\ (9d),\ (9e),\ (9f),\ (9g). \tag{22c}$$

We find that (22a) and (22b) are non-convex. To deal with the non-convex expression $R_{b,m}[n]$ in (22a), we split it into a difference of two functions as

$$R_{b,m}[n] = R_{b,m,1}[n] - R_{b,m,2}[n]. \tag{23}$$

By defining $\eta_m[n] = \frac{\|\mathbf{u}[n]-\mathbf{b}_m\|^2+H^2}{p[n]}$, $R_{b,m,1}[n]$ and $R_{b,m,2}[n]$ are expressed as

$$R_{b,m,1}[n] = \log_2\left(\frac{\beta_0^2}{\delta_m[n] d_0^{\alpha}} + \frac{\mu\beta_0}{\eta_m[n]} + \sigma^2\right), \tag{24}$$

$$R_{b,m,2}[n] = \log_2\left(\frac{\mu\beta_0}{\eta_m[n]} + \sigma^2\right). \tag{25}$$

$R_{b,m,1}[n]$ is convex with $\delta_m[n]$ and $\eta_m[n]$. Similar to (15), we can define $\eta_m^r[n] = \frac{\|\mathbf{u}^r[n]-\mathbf{b}_m\|^2+H^2}{p^r[n]}$, and acquire its lower bound as

$$R_{b,m,1}[n] \geq E^r_{m,1}[n] + F^r_{m,1}[n]\left(\delta_m[n] - \delta^r_m[n]\right) + G^r_{m,1}[n]\left(\eta_m[n] - \eta^r_m[n]\right) = R^{lb}_{b,m,1}[n], \tag{26}$$

where

$$E^r_{m,1}[n] = \log_2\Big(\frac{\beta_0^2}{\delta^r_m[n] d_0^\alpha} + \frac{\mu\beta_0}{\eta^r_m[n]} + \sigma^2\Big), \tag{27}$$

$$F^r_{m,1}[n] = -\frac{\frac{\beta_0^2}{(\delta^r_m[n])^2 d_0^\alpha}\log_2 e}{\frac{\beta_0^2}{\delta^r_m[n] d_0^\alpha} + \frac{\mu\beta_0}{\eta^r_m[n]} + \sigma^2}, \tag{28}$$

$$G^r_{m,1}[n] = -\frac{\frac{\mu\beta_0}{(\eta^r_m[n])^2}\log_2 e}{\frac{\beta_0^2}{\delta^r_m[n] d_0^\alpha} + \frac{\mu\beta_0}{\eta^r_m[n]} + \sigma^2}. \tag{29}$$

To handle the non-convex $R_{b,m,2}[n]$, slack variables $\mathbf{S}=\{S_m[n], m \in \mathcal{M}, n \in \mathcal{N}\}$ are introduced, which satisfy

$$S_m[n] \leq \frac{\|\mathbf{u}[n] - \mathbf{b}_m\|^2 + H^2}{p[n]} = \eta_m[n]. \tag{30}$$

Since $\eta_m[n]$ is convex, its lower bound can be given as

$$\eta_m[n] \geq \eta^r_m[n] + 2\Big(\frac{\mathbf{u}^r[n] - \mathbf{b}_m}{p^r[n]}\Big)^T(\mathbf{u}[n] - \mathbf{u}^r[n]) - \frac{\|\mathbf{u}^r[n] - \mathbf{b}_m\|^2 + H^2}{(p^r[n])^2}(p[n] - p^r[n]) = \eta^{lb}_m[n]. \tag{31}$$

Thus, the constraint in (30) is approximately rewritten as

$$S_m[n] \leq \eta^{lb}_m[n]. \tag{32}$$

Similar to Subsection III.B, (22b) can be approximated by the lower bound in (18). According to the above derivations, (22) can be approximately expressed as

$$\max_{\mathbf{P},\mathbf{U},\mathbf{S}} \ \min_m \frac{1}{N}\sum\nolimits_{n=1}^{N} R^{lb}_{b,m,1}[n] - \log_2\Big(\frac{\beta_0}{S_m[n]} + \sigma^2\Big) \tag{33a}$$

$$s.t. \ \ \frac{1}{N}\sum\nolimits_{n=1}^{N} \hat{\theta}_k[n] R^{lb}_{w,k}[n] \geq R_0, \ k \in \mathcal{K}, \tag{33b}$$

$$S_m[n] \leq \eta^{lb}_m[n], \ m \in \mathcal{M}, n \in \mathcal{N}, \tag{33c}$$

$$(9c), \ (9d), \ (9e), \ (9f), \ (9g). \tag{33d}$$

(33) is convex and can be tackled via CVX.

D. Iterative Algorithm

According to the analysis in the previous subsections, we propose a three-stage iterative algorithm by solving the convex sub-problems (11), (21) and (33) alternately, which is summarized in Algorithm 1. Then, the binary variables $\theta_k[n]$ is recovered from $\hat{\theta}_k[n]$ in the following way

$$\theta_k[n] = \begin{cases} 1 & \text{if} \quad k = \underset{i\in\{1,\cdots,K\}}{\arg\max}\ \hat{\theta}_i[n], \\ 0 & \text{else.} \end{cases} \tag{34}$$

In Algorithm 1, the main computational complexity originates from solving three convex sub-problems in Step 3, Step 4 and Step5. In Step 3, a linear programming is solved by the interior-point method with the computational complexity $\mathcal{O}\big(L_1\sqrt{KN}\big)$, L_1 is the iteration number for updating the user scheduling. For Step 4 and Step 5, both (21) and (33) have the logarithmic form. By employing interior-point method, the computational complexity for Step 4 and Step 5 is given as $\mathcal{O}\big(L_2(3N)^{3.5}\big)$ and $\mathcal{O}\big(L_3(3N+MN)^{3.5}\big)$, respectively. L_2 and L_3 are the number of iterations for solving (21) and (33), respectively. Thus, the overall computational complexity is $\mathcal{O}\left(L_4\big(L_1\sqrt{KN} + L_2(3N)^{3.5} + L_3(3N+MN)^{3.5}\big)\right)$, with L_4 being the iteration number. Since the object value is non-decreasing in each iteration, and it is upper-bounded by its optimal value, the proposed algorithm converges, although it is not guaranteed to converge to the optimal solution.

Algorithm 1 Iterative algorithm for (9).

1: Initialize feasible $\mathbf{P}^0$ and $\mathbf{U}^0$, and let $r = 0$.
2: **repeat**
3: Solve (11) via $\mathbf{P}^r$ and $\mathbf{U}^r$, and obtain the optimized solution $\hat{\mathbf{\Theta}}^{r+1}$.
4: Solve (21) via $\hat{\mathbf{\Theta}}^{r+1}$, and obtain the pre-optimized solution $\bar{\mathbf{P}}^{r+1}$ and $\bar{\mathbf{U}}^{r+1}$.
5: Solve (33) via $\hat{\mathbf{\Theta}}^{r+1}$, $\bar{\mathbf{P}}^{r+1}$ and $\bar{\mathbf{U}}^{r+1}$, and obtain the optimized solution $\mathbf{P}^{r+1}$ and $\mathbf{U}^{r+1}$.
6: Update $r = r + 1$.
7: **until** the increase of the objective value is below a threshold $\varepsilon > 0$

IV. Simulation Results and Discussion

In the simulation, 4 ground users and 3 pairs of ambient backscatter users are distributed in a square area of 2000 × 2000 m^2. We set H = 50 m, D = 100 m, N = 50, T = 100 s, σ^2 = -120 dBm, μ = 10^{-5}, α = 2.7, and $\varepsilon = 2 \times 10^{-4}$. A fixed distance d_0 is set as 10 m because long distance will lead to low backscatter rate. The initial trajectory is a circle with the geometric center of all the ground nodes as its horizontal circle center, and the average distance between the center and each node is employed as the circle radius. The initial transmit power of UAV is $p[n] = p_0, n \in \mathcal{N}$.

The convergence of the proposed algorithm with different p_0 is shown in Fig. 2, where R_0 = 1 bit/s/Hz. The scheme of no coarse optimization is also demonstrated for comparison. Note that unlike in (7), in Fig. 2 and the following Fig. 4, the interference from other backscatter pairs is considered. It is observed that the average backscatter rate increases with iterations. The proposed algorithm converges when the number of iterations is about 20. Without coarse optimization, nearly 40 iterations are required. This is because the coarse optimization process guarantees that the trajectory is close to the backscatter users to improve SNR. Moreover, the data rate of AmBC is low. Since the practical application scenarios in AmBC includes smart hand-held devices, vehicular communicators and RFID tags, low data rate is sufficient to meet their requirements.

The optimized UAV trajectories with different rate threshold are shown in Fig. 3. The average transmit power p_0 = 100 mW. The results indicates that our proposed algorithm can successfully improve the UAV trajectory. In addition, when R_0 = 1 bit/s/Hz, the UAV has the chance to stay above the AmBC users to achieve higher backscatter rate. As R_0 increases, the

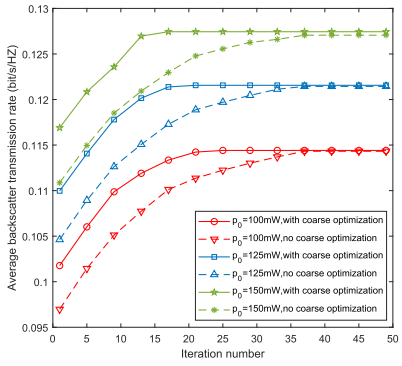

Fig. 2. Convergence speed of the proposed algorithm under different p_0.

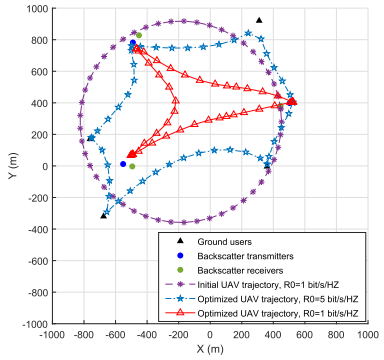

Fig. 3. Initial and optimized UAV trajectories with different R_0.

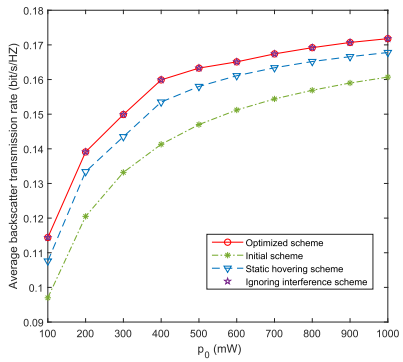

Fig. 4. Average backscatter transmission rate versus different p_0.

UAV is getting closer to the ground users to satisfy their rate requirements. Since the UAV has to serve both the ground users and the AmBC pairs, its trajectory has a tradeoff between the rate of the two kinds of users.

Fig. 4 shows the average backscatter transmission rate with several values of average UAV transmit power p_0, where R_0 = 1 bit/s/Hz. In addition, three benchmark schemes are introduced for comparison: 1) Initial scheme; 2) Static hovering scheme, i.e., the UAV hovers at the circular center with the initial transmit power. 3) Ignoring interference, i.e., the interference of AmBC networks is ignored. According to Fig. 4, the proposed scheme achieves higher average backscatter rate than the benchmarks 1) and 2) , especially when p_0 is small. In addition, we can see that the performance gain is negligible when ignoring the interference. The results also show that when p_0 increases, the average transmission rate of AmBC increases. However, little gain can be achieved when p_0 is large enough. From (8c), We can observe that both the backscatter signal and the interference are originated from the UAV. This case reveals that the investigated AmBC system is interference limited at high SNR regime.

V. Conclusions

In this correspondence, the rate maximization of a UAV-assisted AmBC system has been investigated, where the user scheduling, UAV transmit power and trajectory are jointly optimized. To address this complicated optimization problem, a three-stage iterative algorithm has been designed. The user scheduling has been approximately solved in the first stage. To accelerate the convergence, a coarse optimization scheme has been proposed to obtain a preliminary transmit power and trajectory. The third stage is a fine optimization scheme. The results have shown that our proposed scheme can efficiently enhance the average backscatter rate.

References

[1] N. Zhao, W. Lu, M. Sheng, Y. Chen, J. Tang, F. R. Yu, and K. Wong, "UAV-assisted emergency networks in disasters," *IEEE Wireless Commun.*, vol. 26, no. 1, pp. 45–51, Feb. 2019.

[2] S. Eom, H. Lee, J. Park, and I. Lee, "UAV-aided wireless communication designs with propulsion energy limitations," *IEEE Trans. Veh. Technol.*, vol. 69, no. 1, pp. 651–662, Jan. 2020.

[3] R. Zhang, X. Pang, J. Tang, Y. Chen, N. Zhao, and X. Wang, "Joint location and transmit power optimization for NOMA-UAV networks via updating decoding order," *IEEE Wireless Commun. Lett.*, vol. 10, no. 1, pp. 136–140, Jan. 2021.

[4] A. Li, Q. Wu, and R. Zhang, "UAV-enabled cooperative jamming for improving secrecy of ground wiretap channel," *IEEE Wireless Commun. Lett.*, vol. 8, no. 1, pp. 181–184, Feb 2019.

[5] T. Shui, J. Hu, K. Yang, H. Kang, H. Rui, and B. Wang, "Cell-free networking for integrated data and energy transfer: Digital twin based double parameterized DQN for energy sustainability," *IEEE Trans. Wireless Commun.*, 2023, to appear.

[6] Y. Zhao, Y. Wu, J. Hu, and K. Yang, "A general analysis and optimization framework of time index modulation for integrated data and energy transfer," *IEEE Trans. Wireless Commun.*, vol. 22, no. 6, pp. 3657–3670, Jun. 2023.

[7] X. Lu, D. Niyato, H. Jiang, D. I. Kim, Y. Xiao, and Z. Han, "Ambient backscatter assisted wireless powered communications," *IEEE Wireless Commun.*, vol. 25, no. 2, pp. 170–177, Apr. 2018.

[8] R. Duan, X. Wang, H. Yigitler, and et al., "Ambient backscatter communications for future ultra-low-power machine type communications: Challenges, solutions, opportunities, and future research trends," *IEEE Commun. Mag.*, vol. 58, no. 2, pp. 42–47, Feb. 2020.

[9] G. Yang, R. Dai, and Y.-C. Liang, "Energy-efficient UAV backscatter communication with joint trajectory design and resource optimization," *IEEE Trans. Wireless Commun.*, vol. 20, no. 2, pp. 926–941, Feb. 2021.

[10] D.-H. Tran, S. Chatzinotas, and B. Ottersten, "Throughput maximization for backscatter- and cache-assisted wireless powered UAV technology," *IEEE Trans. Veh. Technol.*, vol. 71, no. 5, pp. 5187–5202, May. 2022.

[11] M. Hua, L. Yang, C. Li, Q. Wu, and A. L. Swindlehurst, "Throughput maximization for UAV-aided backscatter communication networks," *IEEE Trans. Commun.*, vol. 68, no. 2, pp. 1254–1270, Feb. 2020.

[12] R. Han, L. Bai, Y. Wen, J. Liu, J. Choi, and W. Zhang, "UAV-aided backscatter communications: Performance analysis and trajectory optimization," *IEEE J. Sel. Areas Commun.*, vol. 39, no. 10, pp. 3129–3143, Oct. 2021.

[13] J. Wang, S. Xu, S. Han, and L. Xiao, "UAV-powered multi-user intelligent reflecting surface backscatter communication," *IEEE Trans. Veh. Technol.*, vol. 72, no. 8, pp. 10 251–10 262, Aug. 2023.

[14] S. Yang, Y. Deng, X. Tang, Y. Ding, and J. Zhou, "Energy efficiency optimization for UAV-assisted backscatter communications," *IEEE Commun. Lett.*, vol. 23, no. 11, pp. 2041–2045, Nov. 2019.

[15] J. Hu, X. Cai, and K. Yang, "Joint trajectory and scheduling design for UAV aided secure backscatter communications," *IEEE Wireless Commun. Lett.*, vol. 9, no. 12, pp. 2168–2172, Dec. 2020.

[16] X. Jiang, M. Sheng, N. Zhao, J. Liu, D. Niyato, and F. Richard Yu, "Outage analysis of UAV-aided networks with underlaid ambient backscatter communications," *IEEE Trans. Wireless Commun.*, 2023, to appear.

[17] X. Lin, V. Yajnanarayana, S. D. Muruganathan, S. Gao, H. Asplund, H.-L. Maattanen, M. Bergstrom, S. Euler, and Y.-P. E. Wang, "The sky is not the limit: LET for unmanned aerial vehicles," *IEEE Commun. Mag.*, vol. 56, no. 4, pp. 204–210, Apr. 2018.

[18] A. Varshney, O. Harms, C. Pérez-Penichet, C. Rohner, F. Hermans, and T. Voigt, "Lorea: A backscatter architecture that achieves a long communication range," in *Proc. ACM SenSys'17*. Delft, Netherlands, 2017.